Numerical Simulations of a High Frequency Switching 4/2 ON/OFF Valve for Pulse Modulation Switching Digital Circuits

Francesco Sciatti[1*], Paolo Tamburrano[1], Andrew R. Plummer[2], Elia Distaso[1], Pietro De Palma[1] and Riccardo Amirante[1]

[1] Department of Mechanics, Mathematics and Management (DMMM), Polytechnic University of Bari, 70121 Bari, Italy;

[2]Centre for Power Transmission and Motion control (PTMC), University of Bath, Bath BA2 7AY, UK;

**Corresponding author: francesco.sciatti@poliba.it*

Abstract.

Proportional valves and servovalves are employed in several industrial and aeronautical applications. However, both employ sliding spools, which cause high power consumption, essentially due to the large pressure drops across the metering orifices. A recent research field aims to substitute spool valves with ON/OFF valves that have high switching frequency and produce low pressure drops, in order to drastically reduce such high-energy dissipations. The aim of this paper is to evaluate the performance of a novel high frequency switching four-way two-position (4/2) ON/OFF valve actuated directly by a commercially available multilayer piezoelectric actuator, called ring stack. To this end, well-established equations, implemented in Simulink by means of the libraries of Simscape Fluids, are used. The proposed architecture shows simplicity of construction; in addition, very effective flow modulation along with low pressure drops and high flow rates are predicted by the simulations.

Keywords. Piezoelectric Actuators, Spool Valves, Digital Hydraulics, ON/OFF Valves, Simulink.

1. INTRODUCTION

Analog hydraulic valves, both proportional valves and servovalves, have extensively been used in lots of industrial and aeronautical applications for several decades [1], [2], [3]. The basic function of these valves is to control the oil flow delivered to an actuator by changing the opening of the valve metering orifices by means of the main spool displacement [4], [5], [6]. Additionally, these control components are crucial in pneumatic systems, such as in vital biomedical equipment like lung ventilators for intensive care units, regulating patient gas

inhalation and exhalation [7]. However, the use of proportional and servovalves is not energy efficient since both employ sliding spools, which cause high throttling losses in the system [8], [9]. In a previous study by the authors of this paper, a power dissipation equal to 7 kW was evaluated for a medium size spool valve considering a pressure drop of 60 bar and a flow rate of 60 L/min [10]. In addition, the correct operation of spool valves can easily be hindered by oil contamination [4], [5].

A recent research field aims to substitute commercially available spool valves, both proportional and servovalves, with the digital hydraulic technology by means of the use of low-cost ON/OFF valves in order to reduce the energy consumption and increase the efficiency of the system [11], [12], [13]. Higher reliability, lower energy consumption, more precision in machine motions, fewer shutdowns, less loss of production, lower original investment and spare parts carrying costs are among the benefits [14], [15]. Moreover, the digital hydraulic technology directly adopts digital signals to control valves without D/A conversion, which simplifies the control mode and removes the noise sensitivity typical of servovalves [16].

A standard definition of digital hydraulics is provided in [16], namely, “a system which controls a discrete fluid with a modulated, discrete, digital signal directly to realize active and intelligent control of the system output”.

The digital hydraulic technology can be divided into two main categories; in the first type, the hydraulic circuit is composed of a large number of parallel – connected on/off valves; in the second type, the hydraulic circuit is based on high frequency switching technologies [16]. The two types of digital hydraulic circuits are shown in Figure 1 and Figure 2.

The circuit shown in Figure 1 is called Digital Flow Control Unit (DFCU). In this system, the Pulse Code Modulation (PCM) approach is used. In particular, a precise flow control can be obtained through the encoding control of several robust ON/OFF valves connected in parallel. Thus, if more precise flow rates are required, more ON/OFF valves need to be used. In the DFCU circuit, the ON/OFF valve is normally a closed two-way two-position valve, which blocks flow when it is in the unactuated position and passes flow when actuated. If there are N switching valves in the circuit, there will be 2^N possible combinations, thus, by turning the valves on and off, the individual valve flows are combined to form a total flow using a binary table. The main issue of this approach is that numerous ON/OFF valves are needed and must be actuated at the same time, necessitating a precise timing of each individual valve.

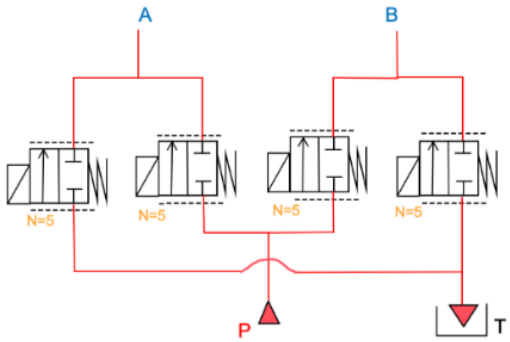

Figure 1. Digital Flow Control Unit (DFCU) circuit with simplified drawing symbol, where N represents the number of ON/OFF valves.

Because these valves are ON/OFF, they do not require a spool adjusting flow and can have the same architecture as that of poppet valves. A poppet valve is capable of performing several working cycles with lower pressure drops than proportional valves because the flow area can be designed larger [14].

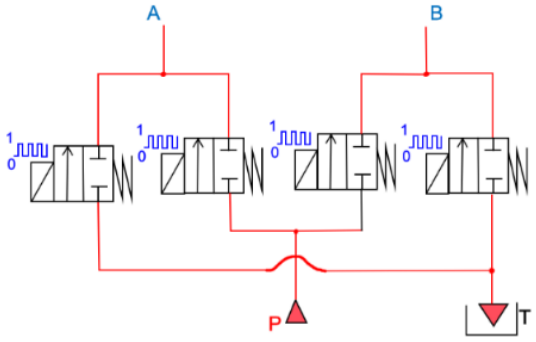

Figure 2. Pulse Modulation Switching (PMS) digital circuit using four 2/2 ON/OFF valves.

The circuit depicted in Figure 2 is called Pulse Modulation Switching (PMS) digital circuit. The ON/OFF valves used in this circuit are the same as those used in the DFCU circuit, apart from being larger. High frequency switching controlled valves allow the average flow area to be adjusted by the Pulse Width Modulation (PWM) technique. In particular, a pulse signal (from 0 to 1) is delivered to the digital valve and flow modulation is obtained by changing the frequency of the pulse signal. The switching frequency has an impact on the controllability: the lower the frequency, the higher the controllability obtained. However, a low frequency increases the pressure pulsation. Accumulators and inertance tubes are normally used to suppress noise and smooth the flow rate obtained [17], [18]. A PMS digital circuit can be considered the better solution since it requires fewer valves than those employed in a DFCU circuit.

Considerable research has been done in the past decades into the development of digital valves. The basis for the design of such devices is to create a rapid switch from fully open to fully closed position in less than 5 ms with very small pressure losses.

Regarding the PCM approach, Bower's invention, issued in 1961, is the first to use real PCM control with a dual-acting actuator [19]. However, the most general PCM valve system was presented by Murphy and Weil in 1962 [20]. In this system, each flow line has its own ON/OFF valve series, allowing for meter-in and meter-out flow control. Despite the fact that the PCM method and its modifications have actively been patented in the field of hydraulics, only few articles appear in the literature [21], [22].

Regarding the PWM approach, various high frequency switching digital valves were studied and developed by several researchers [23], [24], [25]. These valves presented very fast response, but the flow rates were limited to low flow applications. Because of this, apart from very small circuits, digital hydraulics has yet to find practical applications.

In this scenario, this paper proposes a novel high frequency switching 4/2 ON/OFF valve architecture that can be manufactured and used in the digital hydraulic circuit shown in Figure 3, in order to replace proportional and servovalves in aeronautical and industrial applications. PMS digital circuits are usually proposed to be equipped with 2/2 ON/OFF valves. In the present paper, it is proposed to use 4/2 ON/OFF valves in order to reduce the number of the components, as shown in Figure 3.

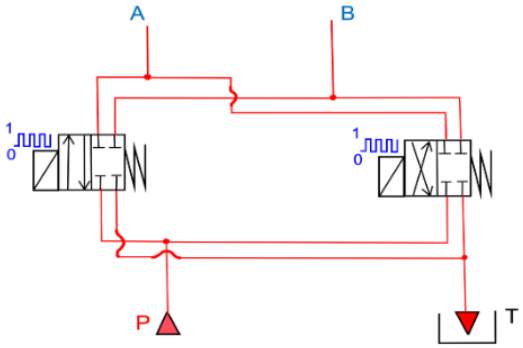

Figure 3. Pulse Modulation Switching (PMS) digital circuit using two 4/2 ON/OFF valves.

The idea here investigated thoroughly consists in using a commercially available multilayer piezoelectric actuator, called ring stack, to move two inner poppets in the 4/2 poppet valve. This idea was partially presented in [10], where a feasibility study of a high frequency switching 2/2 ON/OFF valve was performed using a simplified Simulink model in order to predict simple open-loop step tests. In this paper, the investigation regards the 4/2 valve, and a more complete assessment is performed using a more detailed Simulink model, which is now able to simulate closed loop control.

The PWM technique is proposed to be used. In particular, by changing the duty cycle of the input pulse voltage (V_c), different values of the average flow rate (Q_{mean}) can be obtained. The duty cycle, denoted by *%DC*, is the ratio of the pulse duration (Δt_{on}) to the overall period of the input signal (τ). The latter is kept constant; therefore, the duty cycle ($\%DC = \Delta t_{on}/\tau$) is changed from 0 to 1 and is expressed as a percentage, i.e. from 0% to 100%.

Firstly, the valve architecture is presented. Then, the improved Simulink model is described. After that, the simulation results obtained through open and closed loop control are presented and discussed. The findings allow one to understand the benefits and drawbacks, which are finally summarised in the conclusions.

2. VALVE LAYOUT

In this section, the valve layout is analysed. The main component of this architecture is the ring stack actuator. It consists of a series of piezoelectric ring elements stacked one on top of the other and enclosed between two electrodes. The thickness of the layers is of the order of 25–100 μm. Various combinations of maximum free stroke and blocking force can be obtained depending on the height of the stack. The blocking force is the maximum actuation force and is obtained when the actuator is blocked from moving and when the maximum operating voltage is applied; the maximum free stroke is the maximum displacement ideally achievable for a null actuation force, i.e., when the actuator experiences no resistance to movement, and when the maximum voltage is applied. The ring stack with the maximum height (200 mm) produced by Noliac is adopted in the numerical simulations, namely, model NAC2125-HXX [26]. In Table 1, its main characteristics are shown.

Table 1. NAC2125-HXX RING STACK: Specifications [26].

Parameter	Symbol	Unit	Value
Length/outer diameter	d_o	mm	20
Width/ inner diameter	d_i	mm	12
Height	H	mm	200
Max. operating voltage	V_{max}	V	200
Max. free stroke	x_{max}	μm	325
Max. blocking force	$F_{b,max}$	N	8450
Capacitance	C_{ap}	nF	79300
Stiffness	k_p	N/m	$26 \cdot 10^6$

A feasibility study of a 2/2 poppet-type valve based on the use of the same piezo actuator was performed in [10]. In order to reduce the number of valves from four to two and, thus reducing the complexity of the system, a novel 4/2 poppet-type valve architecture, shown in Figure 4, is now presented. The valve, in order to be employed in the digital circuit shown in Figure 3, must meet the following targets:

- it must switch between open and closed in a very short time interval, i.e., less than 5 ms;
- it must generate low pressure drops even for high flow rates. A real goal is to achieve a maximum pressure drop of 20 bar at 60 L/min;
- it must be robust, since it must switch numerous times a day.

In the novel 4/2 valve architecture, shown in Figure 4, the ring stack actuator (1) allows the poppets (2) to be moved. The latter, which are inserted through the hole of the stack (3), are kept in contact with the piezo actuator by means of a spring (4) which in turn ensures a correct pre-compression (δ_0) to the ring stack. Indeed, since the piezo stack actuator cannot withstand large pulling forces, a preload must be applied to avoid damage. It has widely been proved that a correct value of preload grants a longer lifetime for this type of piezoelectric actuator [27]. In particular, the values for the optimum preload range from 20 to 50 percent of the blocking force [28]. When a differential voltage is applied to the ring-stack, the poppets are moved from their seat and flow is allowed from Port P to Port A, and from Port B to Port T. Taking advantage of the rapid response of the piezoelectric actuator

as well as the simplicity of the valve architecture, this valve has the potential to satisfy the previously specified targets.

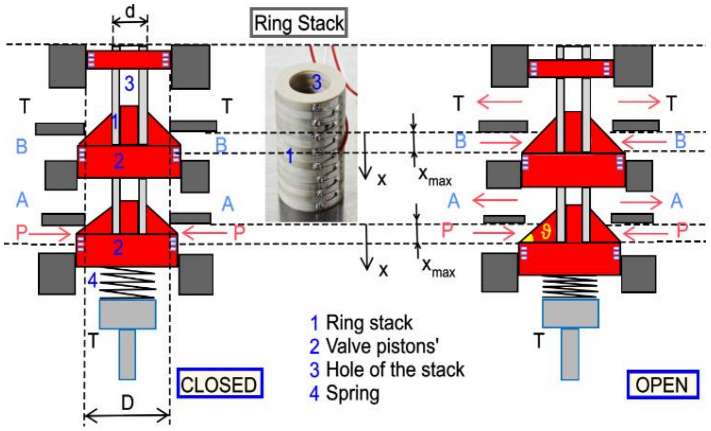

Figure 4. Proposed 4/2 poppet-type valve architecture: closed position (left), open position (right).

3. SIMULINK MODEL

A numerical model simulating the performance of the valve concept, shown in Figure 4, has been developed. The equations of the numerical model, which have been implemented into the Simscape Fluids environment [29], are described in the following.

An amplifier is needed to transform a low input pulse voltage V_c (from 0 to 5 V) into a high output voltage V_{amp} (from 0 to 200 V). A second order transfer function $G(s)$ is used to model the relation between V_{amp} and V_c, as already done in previous studies [10]:

$$G(s) = \frac{V_{amp}}{V_c} = \frac{k_a \omega_n^2}{s^2 + 2\xi\omega_n s + \omega_n^2}, \tag{1}$$

where s is the complex variable, while k_a, ω_n, and ξ are the gain, natural frequency and damping ratio of the amplifier, respectively. In the code, it is possible to model the current limit I_{max}, thus the rate of change of voltage can be limited according to Equation (2):

$$\left(\frac{dV_{amp}}{dt}\right)_{max} = \frac{I_{max}}{C_{ap}}, \tag{2}$$

where C_{ap} is the capacitance of the ring-stack.

The blocking force F_b depends on the amplified voltage V_{amp} as follows:

$$F_b = K_{VF} V_{amp}, \tag{3}$$

where K_{VF} is a conversion factor (from voltage to newton). The blocking force F_b determines the actuation force F_{act}, which can be calculated as follows [26]:

$$F_{act} = F_b - k_p x, \tag{4}$$

where k_p is the stiffness of the actuator and x is the displacement of the poppets.

The equilibrium of the forces acting on the poppets, when the valve is actuated, can be written as follows [10]:

$$F_{act} - k_s(x + \delta_0) - F_{flow} - C\dot{x} - m\ddot{x} = 0, \tag{5}$$

where k_s is the stiffness of the additional spring, which ensures a correct pre-compression δ_0 to the ring stack; F_{flow} is the flow force acting on the poppets'; C and m are the damping factor (accounting for fluid viscosity) and the mass of the moving parts, respectively.

To evaluate the damping factor of the moving parts, which is due to the frictional forces acting on it, the following relation can be used [10]:

$$C = \frac{\mu\pi D_p l_p}{c\sqrt{1 - \left(\frac{\varepsilon}{c}\right)^2}}, \tag{6}$$

where μ is the dynamic viscosity of the oil, D_p and l_p are the diameter and length of the part in contact with the case; c is the radial clearance and ε is the radial eccentricity.

For each metering chamber, the flow forces F_{flow} and the restriction area A_r can be estimated by the following equations [10]:

$$F_{flow} = \rho\frac{Q^2}{A_r}cos\vartheta, \tag{7}$$

$$A_r = \pi D x sin\vartheta, \tag{8}$$

where ρ is the oil density, θ is the poppets' angle equal to the flow angle, D is its effective diameter and Q is the flow rate, which can be calculated as follows [10]:

$$Q = C_D A_r\sqrt{\frac{\Delta p}{\rho}}, \tag{9}$$

where C_D is the discharge coefficient and Δp is the overall pressure drop across the valve. In the model, Port A and Port B are hydraulically connected and the pressure drop $p_A - p_B$ is neglected. Therefore, the pressure drop in Equation (9) becomes:

$$\Delta p = p_P - p_T = 2(p_B - p_T) = 2(p_P - p_A), \tag{10}$$

The values of p_P and p_T are constant input in the model.

The poppets' stroke is confined by two stops which restrict its motion between an upper and a lower bound. Each stop is represented as a spring combined with a damper. When the maximum or minimum displacement is reached, a force F_{stop} which acts on the ring stack can be calculated as [10]:

$$F_{stop} = K_{stop}(x_{max} - x) + C_{stop}\frac{d}{dt}(x_{max} - x), \quad \text{for } x \geq x_{max} \tag{11}$$

$$F_{stop} = K_{stop}(x_{min} - x) + C_{stop}\frac{d}{dt}(x_{min} - x), \quad \text{for } x \leq x_{min}, \tag{12}$$

where K_{stop} and C_{stop} are the spring stiffness and damping of the stop, respectively, with x_{max} and ($x_{min} = 0$) denoting the maximum and minimum displacement of the ring stack.

A block called "Constant Volume Hydraulic Chamber" is used to simulate the volume of oil contained between (P) and (A), and between (B) and (T). This block simulates a fixed-volume chamber with rigid walls while also accounting for fluid compressibility. The following equations are applied [10]:

$$V_{cham} = V_0 + \frac{V_0 p}{E}, \tag{13}$$

$$q_c = \frac{dV_{chamb}}{dt} = \frac{V_0}{E}\frac{dp}{dt}, \tag{14}$$

where V_0 represents the geometrical volume of the chamber (equivalent to the product of an internal diameter D_0 and an overall internal length L_0), V_{cham} represents the oil volume in the chamber at pressure p, and q_c represents the volumetric flow rate through the chamber. The actual bulk modulus E is calculated as follows [10]:

$$E = E_0 \frac{1 + \sigma(\frac{p_a}{p})^{1/\gamma}}{1 + \sigma \frac{{p_a}^{1/\gamma}}{\gamma\, p^{(\gamma+1)/\gamma}} E_o}, \tag{15}$$

where E_0 is the pure liquid bulk modulus, γ is the gas-specific heat ratio (γ = 1.4), σ is the relative gas content at atmospheric pressure and is p_a the atmospheric pressure.

An open-loop control can be simulated in which the duty cycle (*%DC*) of the input pulse voltage V_c can be set, and the output is the mean flow rate Q_{mean}. Alternatively, a closed-loop control can be simulated, in which a proportional–integral (PI) controller adjusts the duty cycle (*%DC*) to obtain the desired mean flow rate according to the calculated error $e(t)$:

$$(\%DC) = K_P e(t) + K_I \int_0^t e(t)dt. \tag{16}$$

where K_P and K_I denote the proportional and integral gain, respectively. The derivative action is not considered in the controller since it is highly sensitive to noise in the process variable signal.

The hysteresis of the ring stack is not simulated. The Simulink solver (Ode 14x) computes the dynamic system's states at successive time steps (0.01 ms) over a specified time span (25 ms), using information provided by the model [29].

4. NUMERICAL RESULTS

The results of the numerical simulations, which concerned both metering chambers of the same valve, i.e., P → A and B → T, are now presented and discussed. The values of the operating parameters are reported in Table 1 (regarding the ring stack actuator) and Table 2 (the system).

Table 2. System parameters assumed for the simulations.

Component	Parameter	Value	Unit
Oil (ISO VG 32)	Temperature (T)	50	[°C]
	Density (ρ)	851	[kg/m^3]
	Viscosity (μ)	0.0187	[kg/(ms)]
Discharge line	Discharge Pressure (p_T)	1	[bar]
Oil chamber volume	Equivalent Diameter (D_0)	60	[mm]
	Equivalent length (L_0)	50	[mm]
	Volume chamber (V_0)	$2 \cdot 10^{-4}$	[m^3]
PiezoValve	Effective poppets' diameter (D)	60	[mm]
	Piston angle (ϑ)	45	[°]
	Length parts contact case (l_p)	50	[mm]
	Eccentricity (ε)	0	[mm]
	Clearance (c)	1	[μm]
	Poppets' damping factor (C)	60	[Ns/m]
	Discharge coefficient (C_D)	0.7	-
	Conversion factor (K_{VF})	42.25	[N/V]
	Stiffness of add. Spring (k_s)	190000	[N/m]
	Pre-compression (δ_0)	8.90	[mm]
	Stop stiffness (K_{stop})	10^8	[N/m]
	Stop Damping (C_{stop})	5000	[Ns/m]
Amplifier	Natural frequency (ω_n)	10000	[rad/s]
	Damping factor (ξ)	1.5	-
	Gain of the amplifier (k_a)	40	-

The proposed setting was used in order to obtain switching times of 5 ms; the average flow rate was modulated by acting on the pulse width of the input signal V_c. Thus, V_c was simulated as a pulse signal from 0 to 5V with a frequency of 200 Hz (overall period τ =5 ms) with variable duty cycle (*%DC*). No current limit was set in the program.

Firstly, the effects of the mass of the moving parts on the system was evaluated. Figure 5 shows open-loop predictions obtained for *%DC*=80% of the input pulse voltage V_c and different values of the mass, namely, *m*=100 g, 150 g and 200 g. In addition to V_c, the time history of the amplified voltage (V_{amp}), of the poppets' position (x), of the flow rate (Q) and of the mean flow rate (Q_{mean}) are plotted. For clarity, the input voltage is multiplied by 20. The graph reveals that the greater the mass, the larger the oscillations of the poppets' position. Since the trend of the flow rate is similar to the trend of the poppets' position, it is important that the mass of the moving parts of the ring stack actuator is taken not too large. In addition, accumulators and an inertance tubes can be used to smooth these oscillations [17], [18]. However, in all the three cases, the average flow rate computed by the program is the same and equal to $Q_{mean} = 53.7$ L/min.

The open loop predictions obtained for Δp=20 bar and *m*=100 g, while considering *%DC*=40%, and *%DC*=70% are shown in Figure 6a and Figure 6b, respectively. Along with the previous quantities, the blocking force (F_b), the actuation force (F_{act}), the current (I) and the mean current (I_{mean}) are plotted. As shown by the graphs, the input pulse voltage (V_c) is converted into a high pulse voltage by the amplifier (V_{amp}) in about 1.5 ms, which in turn is converted into the blocking force (F_b) by means the conversion factor (K_{VF}). The actuation

force (F_{act}), calculated as the difference between the blocking force (F_b) and the internal spring force ($k_p x$), allows the poppets to move and reach a certain position. The poppets oscillate around the achieved position which, however, is not equal to the maximum free stroke (x_{max}) due to the resistance forces, i.e., the force of the additional spring and the flow force. The varying duty cycle results in different values of the mean flow rate: the greater the duty cycle (*%DC*), the greater the average flow rate obtained. In particular, a mean flow rate of 26 L/min and 46 L/min is obtained for a duty cycle equal to 40% and 70%, respectively. In addition, given the rapid response of the high-performance amplifier simulated, the regulation is very effective in all two different scenarios. The simulations also show a large peak of current equal to I =43.5 A, because no current limitation was set in these simulations. However, the peak current only occurs for a brief time, while the mean current is not high ($I_{mean} \approx 6A$).

In Figure 5 and 6, the overall pressure drop across the valve was set to Δp=20 bar, because, as previously explained, the objective is to design a valve which can produce high flow rate with low pressure drops, thus a pressure drop of 10 bar for each metering chamber (P → A and B → T) can be regarded as a right choice, as previously explained.

To evaluate the effects of the flow forces, Figure 7 shows open-loop predictions obtained for different values of Δp (10, 20, 30 bar), while keeping *%DC*=80% and *m*=100 g. As shown in the graph, the higher the overall pressure drop, the greater the mean flow rate obtained. In addition, as the pressure drop across the valve increases, the generated flow forces increase. However, the increased flow forces do not affect the actuation capability of the ring stack actuator since the flow forces (expressed in N in the graph) are much lower than the actuation force (expressed in hN in the graph) in all the three cases examined, as shown in Figure 7b. Thus, the three curves of the actuation forces are coincident (the same occurs with the position *x* (Figure 7a)).

All the results presented up to this point were obtained through an open-loop control system. However, closed loop control is mandatory in real applications. Thus, closed-loop control was also simulated using a simple PI controller which changes the duty cycle (%DC) of the input control signal (V_c) according to Equation (15) to reach the target average flow rate (set point). The parameters of the PI controller, which were determined with the use of the Ziegler–Nichols method, are K_P = 0.01125 and K_I = 3.6. The back calculation anti-windup method was used.

In order to evaluate the effectiveness of the piezo-valve, step tests have been simulated by imposing different values for the set point. The controlled variable is the average flow rate, whereas the control variable is the duty cycle of the input pulse voltage applied to the ring stack. In these simulated closed-loop step tests, the parameters assumed for the simulations were again those presented in Table 1 (regarding the ring stack) and Table 2 (the system). In addition, the mass of the moving parts and the overall pressure drop across the valve were set equal to Δp=20 bar and *m*=100g, respectively.

Figure 8a and Figure 8b show the time history of the simulated mean flow rate obtained during two step tests, i.e., Q_{mean} =40 L/min and Q_{mean} =55 L/min. As visible in the graphs, the time necessary to reach 90% of the set point (i.e., 90% rise time) is very short, specifically a value lower than 10 ms is registered for Q_{mean} = 40 L/min and for Q_{mean} = 55 L/min.

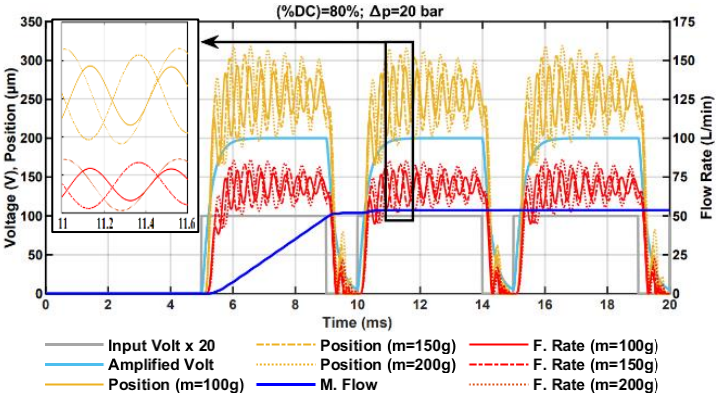

Figure 5. Open loop predictions simulated for (%DC)=80% of the input pulse voltage V_c (from 0 to 5 V) and different values of m (Δp=20 bar): Amplified Voltage (V_{amp}), Poppets' Position (x) , Mean Flow (Q_{mean}) and Flow Rate (Q).

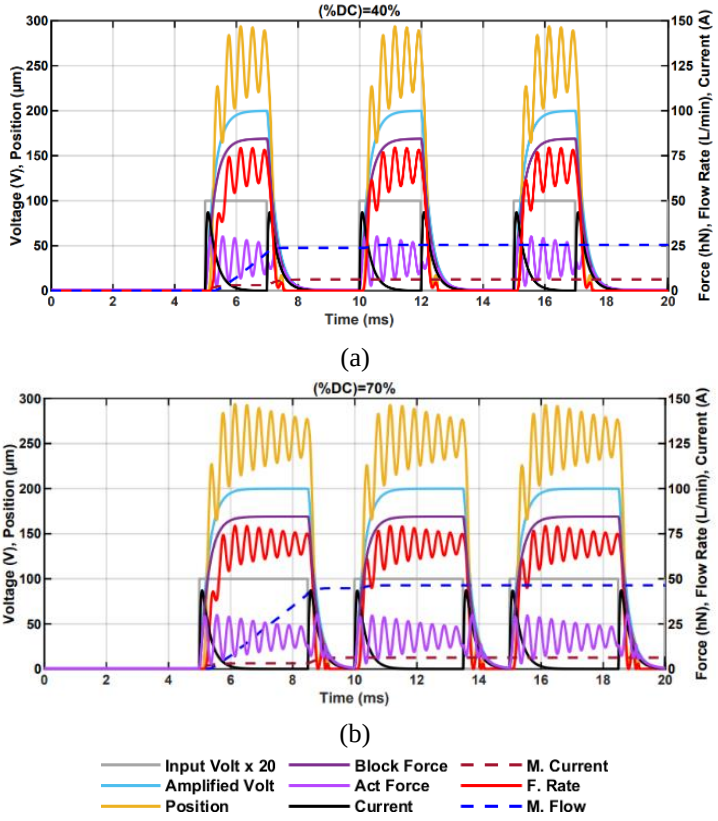

Figure 6. Open loop predictions simulated for two different duty cycles of the input pulse voltage V_c (from 0 to 5 V) (m=100g, Δp=20 bar): (a) ($\%DC$)=40%; (b) ($\%DC$)=70%.

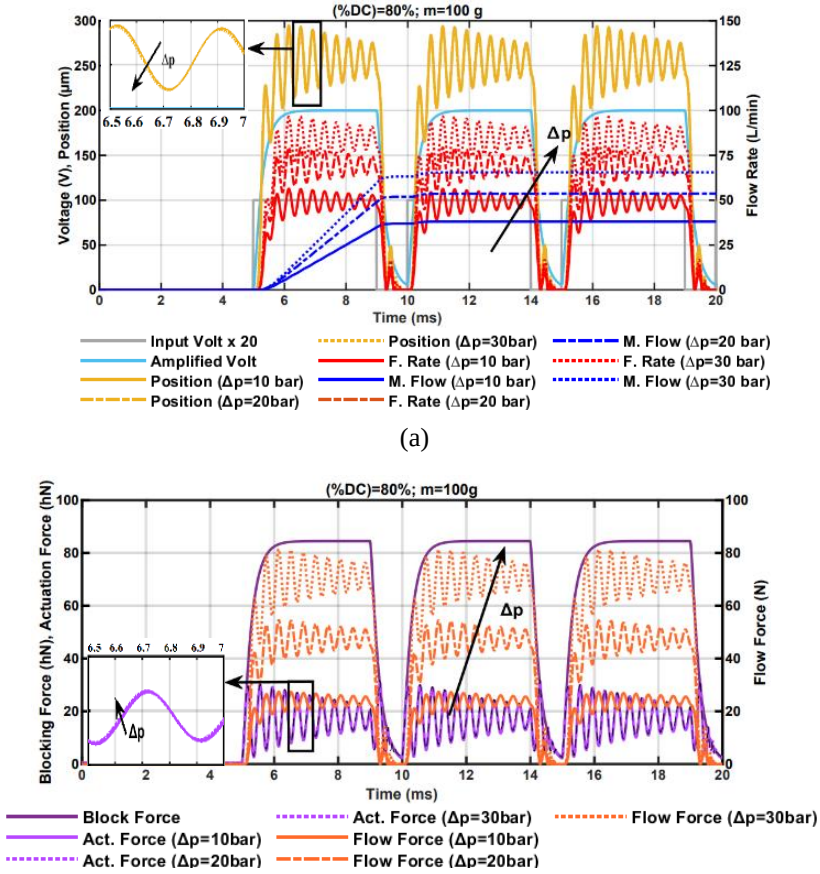

Figure 7. Open loop predictions simulated for (%DC)=80% of the input pulse voltage V_c (from 0 to 5 V) and different values of Δp (m=100g): (a) Amplified Voltage (V_{amp}), Poppets'Position (x), Flow Rate (Q), Mean Flow (Q_{mean}); (b) Blocking Force (F_b), Actuation Force (F_{act}), Flow Force (F_{flow}).

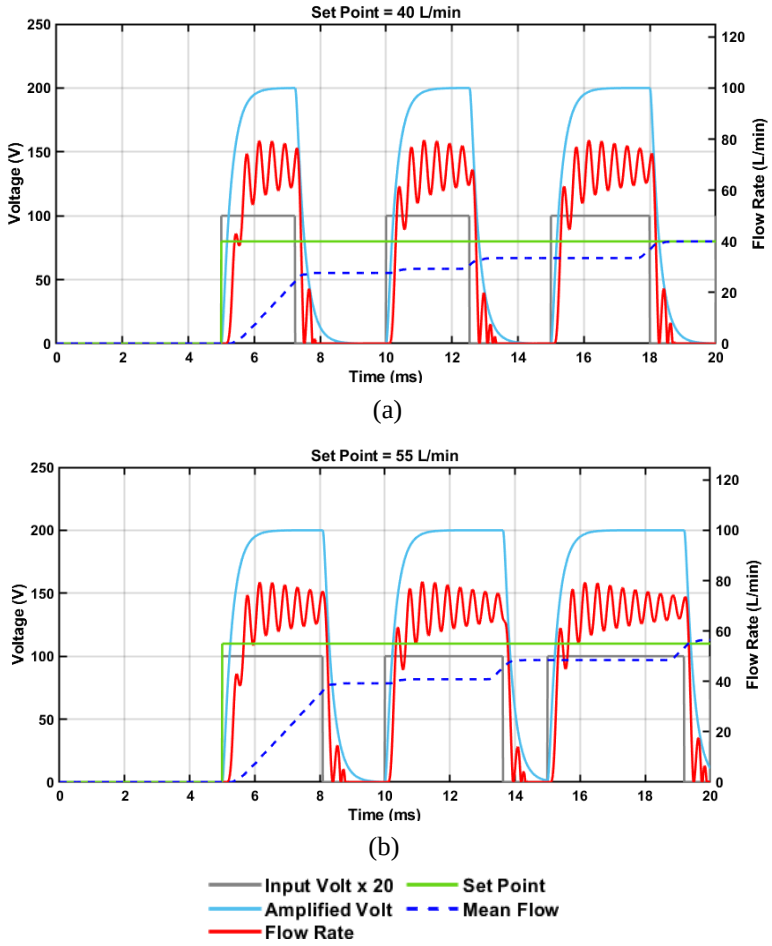

Figure 8. Closed loop results (m=100 g, Δp=20 bar): (a) Q_{mean}=40 L/min; (b) Q_{mean}=55 L/min.

5. CONCLUSIONS

A new fast switching 4/2 ON/OFF valve based on the use of a piezo ring stack was proposed. The piezovalve has characteristics comparable to proportional and servovalves, thus it offers new possibilities for utilizing digital hydraulics in different industrial and aeronautical implementations.

The performance of the new valve architecture was evaluated using detailed and well-established equations implemented in a Simulink code. Firstly, the results obtained with an open-loop control system were presented: by changing the duty cycle of the input pulse voltage, it was possible to change the average flow obtained through the valve. The simulations showed that the control strategy is very effective: an average flow rate of 53.7 L/min was obtained for (*%DC*)=80%, an overall pressure drop across the valve equal to 20 bar and a mass of the moving parts equal to 100 g.

Afterwards, in order to evaluate the effectiveness of the piezo-valve, the results, obtained with a closed-loop average flow rate, were discussed. The parameters of the closed-loop controller were determined by the Ziegler–Nichols method. It was shown that the interval time necessary to reach 90% of the set point is very short, i.e. lower than 10 ms for 40 L/min and for 55 L/min.

Through both the analysis of the characteristics of the ring stack and the simulation results, it is possible to define the advantages and disadvantages aspects of the proposed architecture. The negative aspects are the large size and the high cost of the ring stack, and the need for a high-performance amplifier. The positive aspects are the simplicity of the architecture, the low pressure drops and the very fast response time.

In conclusion, this paper showed that the use of digital hydraulics in industrial and aeronautical applications is feasible and interesting features can be obtained, such as the low energy consumption.

REFERENCES

[1] Moog, “Proportional and Servo Valve Technology,” 2003.

[2] F. Sciatti, P. Tamburrano, P. De Palma, E. Distaso, and R. Amirante, “Detailed simulations of an aircraft fuel system by means of Simulink,” in *Journal of Physics: Conference Series*, IOP Publishing, 2022, p. 012033.

[3] P. Tamburrano *et al.*, “Fuels systems and components for future airliners fuelled with liquid hydrogen,” in *Journal of Physics: Conference Series*, IOP Publishing, 2022, p. 012041.

[4] P. Tamburrano, A. R. Plummer, E. Distaso, and R. Amirante, “A Review of Electro-Hydraulic Servovalve Research and Development,” *International Journal of Fluid Power*, Apr. 2019, doi: 10.13052/ijfp1439-9776.2013.

[5] P. Tamburrano, A. R. Plummer, E. Distaso, and R. Amirante, “A review of direct drive proportional electrohydraulic spool valves: Industrial state-of-the-art and research advancements,” *Journal of Dynamic Systems, Measurement and Control, Transactions of the ASME*, vol. 141, no. 2, Feb. 2019, doi: 10.1115/1.4041063.

[6] A. Plummer, “Electrohydraulic servovalves – past, present, and future.,” in *Proc 10th International Fluid Power Conference*, 2016.

[7] P. Tamburrano, F. Sciatti, E. Distaso, L. Di Lorenzo, and R. Amirante, “Validation of a simulink model for simulating the two typical controlled ventilation modes of intensive care units mechanical ventilators,” *Applied Sciences*, vol. 12, no. 4, p. 2057, 2022.

[8] P. Tamburrano, F. Sciatti, A. R. Plummer, E. Distaso, P. De Palma, and R. Amirante, “A review of novel architectures of servovalves driven by piezoelectric actuators,” *Energies (Basel)*, vol. 14, no. 16, p. 4858, 2021.

[9] P. Tamburrano, E. Distaso, A. R. Plummer, F. Sciatti, P. De Palma, and R. Amirante, “Direct drive servovalves actuated by amplified piezo-stacks: Assessment through a detailed numerical analysis,” *Actuators*, vol. 10, no. 7, Jul. 2021, doi: 10.3390/act10070156.

[10] P. Tamburrano, P. De Palma, A. R. Plummer, E. Distaso, F. Sciatti, and R. Amirante, “Simulation of a high frequency on/off valve actuated by a piezo-ring stack for digital hydraulics,” in *E3S Web of Conferences*, EDP Sciences, 2021, p. 05008.

[11] R. Scheidl, M. Linjama, and S. Schmidt, “Is the future of fluid power digital?,” *Proceedings of the Institution of Mechanical Engineers, Part I: Journal of Systems and Control Engineering*, vol. 226, no. 6, pp. 721–723, 2012.

[12] P. Achten, M. Linjama, R. Scheidl, and S. Schmidt, “Discussion: Is the future of fluid power digital?,” *Proceedings of the Institution of Mechanical Engineers, Part I: Journal of Systems and Control Engineering*, vol. 226, no. 6, pp. 724–727, 2012.

[13] M. S. A. Laamanen and M. Vilenius, “Is it time for digital hydraulics,” in *The eighth Scandinavian international conference on fluid power*, 2003.

[14] Vemet forward, “https://www.valmet.com/media/articles/up-andrunning/ newtechnology/FPDigHydr/.”

[15] M. Linjama, “DIGITAL FLUID POWER-STATE OF THE ART,” 2011.

[16] Q. Zhang, X. Kong, B. Yu, K. Ba, Z. Jin, and Y. Kang, “Review and development trend of digital hydraulic technology,” *Applied Sciences (Switzerland)*, vol. 10, no. 2. MDPI AG, Jan. 01, 2020. doi: 10.3390/app10020579.

[17] M. Pan, N. Johnston, A. Plummer, S. Kudzma, and A. Hillis, “Theoretical and experimental studies of a switched inertance hydraulic system,” *Proceedings of the Institution of Mechanical Engineers, Part I: Journal of Systems and Control Engineering*, vol. 228, no. 1, pp. 12–25, 2014.

[18] C. Yuan, M. Pan, and A. Plummer, “A review of switched inertance hydraulic converter technology,” *J Dyn Syst Meas Control*, vol. 142, no. 5, p. 050801, 2020.

[19] J. L. Bower, “Digital fluid control system.” Google Patents, Sep. 12, 1961.

[20] R. Murphy and J. Weil, “Hydraulic Control System. ,” US Patent No. 3038449., 1962

[21] T. K. Virvalo, “Cylinder speed synchronization,” *Hydraulics & Pneumatics*, vol. 31, no. 12, pp. 55–57, 1978.

[22] A. Laamanen, M. Linjama, J. Tammisto, K. T. Koskinen, and M. Vilenius, “Velocity control of water hydraulic motor,” in *Proceedings of the JFPS International Symposium on Fluid Power*, The Japan Fluid Power System Society, 2002, pp. 167–172.

[23] P. Cui, R. T. Burton, and P. R. Ukrainetz, “Development of a high speed on/off valve,” *SAE transactions*, pp. 312–316, 1991.

[24] J. Yu, X. Han, and Y. Zhang, “Application of high speed digital control solenoid valves in the electronic control of diesel engines,” *Journal of Beijing Institute of Technology*, vol. 14, no. 1, pp. 91–95, 1994.

[25] J. Zhang, M. Yang, and B. Xu, “Design and experimental research of a miniature digital hydraulic valve,” *Micromachines (Basel)*, vol. 9, no. 6, p. 283, 2018.

[26] Noliac. Available online: http://www.noliac.com/products/actuators/ (accessed on 1 March 2022).

[27] M. Fouaidy, M. Saki, N. Hammoudi, and L. Simonet, “Electromechanical characterization of piezoelectric actuators subjected to a variable pre-loading force at cryogenic temperature,” IPN, 2007.

[28] Y. K. Yong, “Preloading piezoelectric stack actuators in high-speed nanopositioning systems,” *Front Mech Eng*, vol. 2, p. 8, 2016.

[29] Guide, Mathworks. Matlab & Simulink. In SimscapeTM User’s R2018a; Mathworks. Natick, MA, USA, 2018.